

## Flavor-singlet mesons in $N_f = 2 + 1$ QCD with dynamical overlap quarks

---

**JLQCD and TWQCD collaborations: T. Kaneko<sup>\*a,b†</sup>, S. Aoki<sup>c,d</sup>, T. W. Chiu<sup>e</sup>, H. Fukaya<sup>f</sup>, S. Hashimoto<sup>a,b</sup>, T. H. Hsieh<sup>g</sup>, J. Noaki<sup>a</sup>, E. Shintani<sup>h</sup> and N. Yamada<sup>a,b</sup>**

<sup>a</sup> KEK Theory Center, High Energy Accelerator Research Organization (KEK), Ibaraki 305-0801, Japan

<sup>b</sup> School of High Energy Accelerator Science, The Graduate University for Advanced Studies (Sokendai), Ibaraki 305-0801, Japan

<sup>c</sup> Graduate School of Pure and Applied Sciences, University of Tsukuba, Ibaraki 305-8571, Japan

<sup>d</sup> Riken BNL Research Center, Brookhaven National Laboratory, Upton, New York 11973, USA

<sup>e</sup> Physics Department, Center for Theoretical Sciences, and Center for Quantum Science and Engineering, National Taiwan University, Taipei, 10617, Taiwan

<sup>f</sup> Department of Physics, Nagoya University, Nagoya 464-8602, Japan

<sup>g</sup> Research Center for Applied Sciences, Academia Sinica, Taipei 115, Taiwan

<sup>h</sup> Department of Physics, Osaka University, Toyonaka, Osaka 560-0043 Japan

We report on our study of flavor-singlet mesons in three-flavor QCD with dynamical overlap quarks. Gauge ensembles are generated on a  $16^3 \times 48$  lattice at a lattice spacing of 0.10 fm with the strange quark masses around its physical value  $m_{s,\text{phys}}$  and up and down quark masses down to  $m_{s,\text{phys}}/5$ . Connected and disconnected meson correlators are calculated using the all-to-all quark propagator. We present our preliminary results on the spectrum of flavor-singlet pseudoscalar and vector mesons.

*The XXVII International Symposium on Lattice Field Theory - LAT2009*

*July 26-31 2009*

*Peking University, Beijing, China*

---

\*Speaker.

†E-mail: takashi.kaneko@kek.jp

## 1. Introduction

A quantitative understanding of interesting properties of the flavor-singlet mesons is an important subject in lattice QCD. The famous  $U(1)$  problem is a long-standing issue albeit past ceaseless efforts. It is also well-known that the flavor-singlet and octet vector mesons mix with each other almost ideally, though this has not yet been confirmed from first principles.

In this article, we report on our study of the flavor-singlet pseudoscalar (PS) and vector mesons. There are two salient features of this work: i) we simulate  $N_f=2+1$  QCD including the effects of dynamical strange quarks, which have been often ignored in previous studies of the flavor-singlet mesons, and ii) we use the all-to-all quark propagator [1] to calculate disconnected meson correlators, which induce the meson mixings and the mass splittings from flavor-non-singlet mesons.

## 2. Simulation method

Our gauge configurations of  $N_f=2+1$  QCD are generated on a  $16^3 \times 48$  lattice using the Iwasaki gauge action and the overlap quark action. We also introduce a topology fixing term [2] into our lattice action to reduce the computational cost, and simulate only the trivial topological sector  $Q=0$  at this stage. The lattice spacing determined from  $F_\pi$  is 0.100(5) fm. We take four values of the degenerate up and down quark masses  $m_l = 0.015, 0.025, 0.035$  and  $0.050$ , which cover a range of the pion mass from 350 to 610 MeV. Two values  $m_s = 0.080$  and  $0.100$  are chosen for the strange quark mass. The physical quark masses fixed from  $M_\pi$  and  $M_K$  are  $m_{l,\text{phys}} = 0.002$  and  $m_{s,\text{phys}} = 0.065$ . Statistics are 2,500 HMC trajectories at each combination of  $m_l$  and  $m_s$ . We refer readers to Ref.[3] for further details on our gauge configurations.

We measure PS and vector meson correlators using the all-to-all quark propagator. For each configuration, we prepare 160 low-lying modes  $(\lambda_m^{(k)}, u^{(k)})$  ( $k=1, \dots, N_e (=160)$ ) of the overlap-Dirac operator  $D(m)$ , where  $m$  is the valence quark mass. Their contribution to the quark propagator is calculated exactly. The higher modes are taken into account stochastically by the noise method. We prepare a single noise vector  $\eta$  for each configuration, and dilute [1] it into  $N_d = 3 \times 4 \times N_t/2$  vectors  $\eta^{(d)}$  ( $d=1, \dots, N_d$ ), which have nonzero elements for a single combination of color and spinor indices and at two consecutive time-slices. The all-to-all propagator can be expressed as

$$D(m)^{-1} = \sum_{k=1}^{N_v} v_m^{(k)} w^{(k)\dagger} \quad (N_v = N_e + N_d) \quad (2.1)$$

with two set of vectors

$$v_m^{(k)} = \left\{ \frac{u^{(1)}}{\lambda_m^{(1)}}, \dots, \frac{u^{(N_e)}}{\lambda_m^{(N_e)}}, x_m^{(1)}, \dots, x_m^{(N_d)} \right\}, \quad w^{(k)} = \left\{ u^{(1)}, \dots, u^{(N_e)}, \eta^{(1)}, \dots, \eta^{(N_d)} \right\}, \quad (2.2)$$

where  $x_m^{(d)}$  is the solution of the linear equation

$$D(m)x_m^{(d)} = (1 - \sum_k u^{(k)} u^{(k)\dagger}) \eta^{(d)}. \quad (2.3)$$

We then construct the following meson field at the temporal coordinate  $t$  with the Dirac matrix  $\Gamma$  and a smearing function  $\phi(\mathbf{r})$

$$\mathcal{O}_{\Gamma, \phi}^{(k,t)}(m;t) = \sum_{\mathbf{x}, \mathbf{r}} \phi(\mathbf{r}) w(\mathbf{x} + \mathbf{r}, t)^{(k)\dagger} \Gamma v_m(\mathbf{x}, t)^{(l)}. \quad (2.4)$$

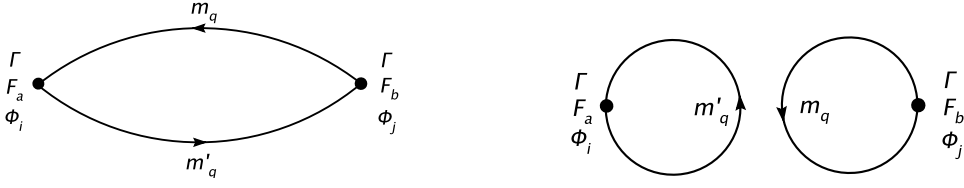


**Figure 1:** Connected (left diagram) and disconnected meson correlators (right diagram). We denote the flavor matrix and the smearing function for the sink meson operator by  $F_a$  and  $\phi_i$ , and those for the source operator by  $F_b$  and  $\phi_j$ . The Dirac matrix is  $\Gamma = \gamma_5$  for PS mesons, whereas we average over  $\Gamma = \gamma_{1,2,3}$  for vector mesons. The masses of propagating quarks are denoted by  $m_{q^{(\nu)}}$ .

The connected and disconnected correlators shown in Fig. 1 can be calculated from these meson fields. The PS meson correlators, for instance, are given by

$$C_{P,ab,ij}(\Delta t) = \frac{1}{N_t} \sum_t \sum_{q,q'=u,d,s} \sum_{k,l=1}^{N_v} (F_a)_{q',q} (F_b)_{q,q'} \mathcal{O}_{\gamma_5, \phi_i}^{(l,k)}(m_q; t + \Delta t) \mathcal{O}_{\gamma_5, \phi_j}^{(k,l)}(m_{q'}; t), \quad (2.5)$$

$$D_{P,ab,ij}(\Delta t) = \frac{1}{N_t} \sum_t \sum_{q'=u,d,s} \sum_{l=1}^{N_v} (F_a)_{q',q'} \mathcal{O}_{\gamma_5, \phi_i}^{(l,l)}(m_{q'}; t + \Delta t) \sum_{q=u,d,s} \sum_{k=1}^{N_v} (F_b)_{q,q} \mathcal{O}_{\gamma_5, \phi_j}^{(k,k)}(m_q; t). \quad (2.6)$$

For simplicity, we often suppress the indices of the smearing functions ( $i$  and  $j$ ) in the following.

In this study, we consider the PS and vector mesons in two different flavor bases: i) light and strange mesons,  $P_{l,s}$  and  $V_{l,s}$ , with their flavor matrices  $F_l = (1/\sqrt{2})\text{diag}[1, 1, 0]$  and  $F_s = \text{diag}[0, 0, 1]$ , and ii) octet and singlet mesons,  $P_{8,0}$  and  $V_{8,0}$ , with  $U(3)$  generators  $T_{8,0}$  for the flavor matrices ( $F_8 = T_8$  and  $F_0 = T_0$ ). We refer to these bases as the light-strange and octet-singlet bases, respectively. The full correlator of these mesons including the disconnected contribution is given by

$$G_{\{P,V\},ab,ij}(\Delta t) = C_{\{P,V\},ab,ij}(\Delta t) - D_{\{P,V\},ab,ij}(\Delta t) \quad (a, b \in \{l, s\} \text{ or } a, b \in \{8, 0\}). \quad (2.7)$$

We calculate all possible correlators with the following five different choices of the smearing function (namely  $i, j = 0, \dots, 4$ )

$$\begin{aligned} \phi_0(\mathbf{r}) &= \delta_{\mathbf{r}, \mathbf{0}}, & \phi_1(\mathbf{r}) &\propto \exp[-0.4|\mathbf{r}|], & \phi_2(\mathbf{r}) &\propto |\mathbf{r}| \exp[-0.4|\mathbf{r}|], \\ \phi_3(\mathbf{r}) &\propto \exp[-1.0|\mathbf{r}|], & \phi_4(\mathbf{r}) &= \text{constant} \end{aligned} \quad (2.8)$$

with the normalization  $\sum_{\mathbf{r}} |\phi_i(\mathbf{r})|^2 = 1$ . The calculation of all these meson correlators is computationally cheap, once we prepare the  $v$  and  $w$  vectors of Eq. (2.2).

Since the quark propagator is decomposed into low- and high-mode contributions, the disconnected correlators can be divided into four contributions, *i.e.*  $D = D^{LL} + D^{LH} + D^{HL} + D^{HH}$ . We calculate these four contributions separately in our measurement.

### 3. Meson correlators

In Fig. 2, we show an example of the light PS and vector meson correlators. We observe that, at relatively small  $\Delta t$ , the disconnected piece  $D_{P,ll}$  is not a large correction to the full correlator  $G_{P,ll}$  and it is dominated by the low-mode contribution  $D_{P,ll}^{LL}$ . Therefore, we may safely ignore the high mode contributions to  $D_{P,ll}$ , namely  $D_{P,ll}^{LH}$ ,  $D_{P,ll}^{HL}$  and  $D_{P,ll}^{HH}$ , to calculate the full correlator as

$$G_{P,ab,ij}^{D=LL}(\Delta t) = C_{P,ab,ij}(\Delta t) - D_{P,ab,ij}^{LL}(\Delta t). \quad (3.1)$$

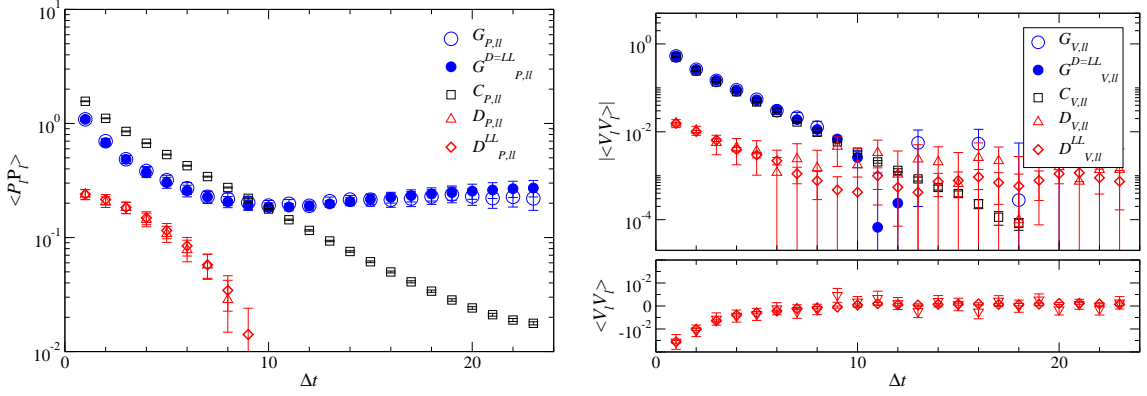


**Figure 2:** Light PS (left panel) and vector meson correlators (right panel) at  $(m_l, m_s) = (0.025, 0.080)$  with exponential smearing  $\phi_1$  for source and sink. Open circles, squares and triangles show the full ( $G_{\{P,V\},ll}$ ), connected ( $C_{\{P,V\},ll}$ ) and disconnected correlators ( $D_{\{P,V\},ll}$ ), respectively. We also plot the low-mode contribution to the disconnected piece  $D_{\{P,V\},ll}^{LL}$  by diamonds, and the full correlator  $G_{\{P,V\},ll}^{D=LL}$  defined in Eq. (3.1) by filled circles. We note that the full PS meson correlator has a constant term as discussed in Section 5.

Figure 2 actually shows that  $G_{P,ll}$  is well approximated by  $G_{P,ll}^{D=LL}$  in the whole region of  $\Delta t$ .

As shown in the same figure, the vector meson full correlator  $G_{V,ll}$  turns out to be noisy at relatively large  $\Delta t$ . The large uncertainty mainly comes from those of high-mode contributions  $D_{V,ll}^{\{LH,HL,HH\}}$  due to the noise method with the small number of noise samples. We observe that  $G_{V,ll}$  at small  $\Delta t$  is well approximated by  $G_{V,ll}^{D=LL}$  defined as in Eq. (3.1), and expect that the high-mode contributions  $D_{V,ll}^{\{LH,HL,HH\}}$  remain to be small at larger  $\Delta t$  since they mainly describe short distance physics. Then  $G_{V,ll}$  is expected to be well approximated by  $G_{V,ll}^{D=LL}$  also at large  $\Delta t$ .

From these observations, we use the meson correlators  $G_{\{P,V\},ab}^{D=LL}$  ignoring the noisy contributions  $D_{\{P,V\},ab}^{\{LH,HL,HH\}}$  to study the spectrum of the flavor-singlet mesons. The superscript “ $D=LL$ ” is suppressed in the following for simplicity.

#### 4. Vector mesons

We plot the vector meson correlators in Fig. 3. In the light-strange basis, the off-diagonal correlators  $G_{V,\{ls,sl\}}$  are about two orders of magnitude smaller than the diagonal ones  $G_{V,\{ll,ss\}}$ . There is no such large hierarchy in  $G_{V,\{88,00,80,08\}}$  in the octet-singlet basis. Since the off-diagonal correlators induce the meson mixing, the above observations indicate that the mixing of the vector mesons is close to the ideal mixing: namely,  $V_8$  and  $V_0$  mesons mix significantly with each other to form  $\omega$  and  $\phi$  mesons, which are well approximated by  $V_l$  and  $V_s$ .

For a more quantitative examination, we solve the generalized eigenvalue problem (GEVP)

$$C(\Delta t')^{-1/2} C(\Delta t) C(\Delta t')^{-1/2} \tilde{u}_n = \tilde{\lambda}_n \tilde{u}_n \quad (n = 0, 1), \quad (4.1)$$

where  $C(\Delta t)$  is  $2 \times 2$  correlator matrix with specified smearing functions for source and sink

$$C(\Delta t) = \begin{pmatrix} G_{V,88}(\Delta t) & G_{V,80}(\Delta t) \\ G_{V,08}(\Delta t) & G_{V,00}(\Delta t) \end{pmatrix}. \quad (4.2)$$

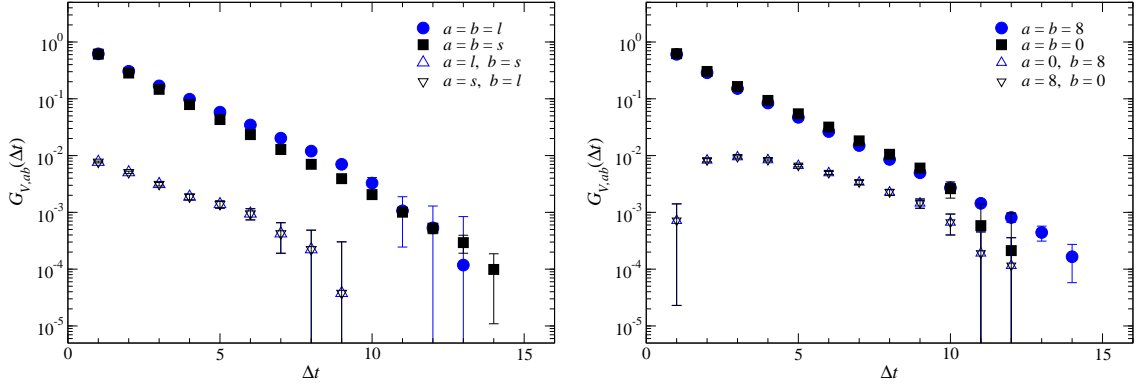


**Figure 3:** Vector meson correlators in the light-strange (left panel) and octet-singlet bases (right panel). Both panels show results with the exponential smearing function  $\phi_1$  at  $(m_l, m_s) = (0.025, 0.080)$ . Filled and open symbols represent diagonal and off-diagonal correlators, respectively.

The creation operators of the energy eigenstates, namely,  $\phi$  and  $\omega$  mesons, are determined from the eigenvectors  $\tilde{u}_n$ . We obtain the following relation for the local operators

$$\begin{cases} \phi = 0.84(5)V_8 - 0.55(7)V_0 = 1.00(1)V_s - 0.04(9)V_l \\ \omega = 0.55(7)V_8 + 0.84(5)V_0 = 0.04(9)V_s + 1.00(1)V_l \end{cases}, \quad (4.3)$$

which implies the ideal mixing of the vector mesons. We observe that this relation of vector meson operators does not change significantly with other choices of the smearing functions.

In Fig. 4, we plot the effective masses of  $\omega$  and  $\phi$  mesons determined from the eigenvalues  $\tilde{\lambda}_n = \exp[-E_n(\Delta t - \Delta t')]$ . By taking a sufficiently large  $\Delta t'$ , the effective masses show small dependence on  $\Delta t$  as well as on the smearing functions. The same figure also shows that  $M_\omega$  and  $M_\phi$  are close to those from the connected correlators of the light and strange mesons  $C_{V,\{ll,ss\}}$ . This is because the diagonal disconnected correlators  $D_{V,\{ll,ss\}}$  are small as seen in Fig. 2, and hence they have small effects to  $M_\omega$  and  $M_\phi$ .

In this analysis, we extrapolate  $M_{\omega(\phi)}$  to the physical point using a simple linear form

$$M_{\omega(\phi)} = a_{\omega(\phi)} + b_{\omega(\phi)}m_l + c_{\omega(\phi)}m_s. \quad (4.4)$$

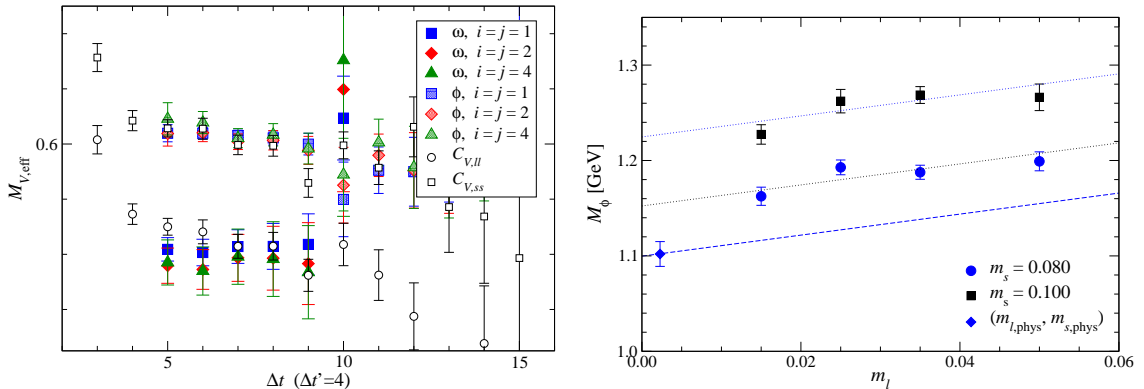


**Figure 4:** Left panel: effective masses of  $\omega$  (solid symbols) and  $\phi$  mesons (shaded symbols) at  $(m_{ud}, m_s) = (0.025, 0.080)$ . We also plot effective masses of  $C_{V,ll}$  (open circles) and  $C_{V,ss}$  (open squares). Right panel: chiral extrapolation of  $M_\phi$ . Dotted and dashed lines show fit lines at  $m_s$  and  $m_{s,\text{phys}}$ , respectively.

As shown in Fig. 4, this fit describes our data reasonably well with  $\chi^2/\text{d.o.f} \sim 1.3$ . We obtain  $M_\omega = 909(25)_{\text{stat}}(-98)_{\text{sys}}$  MeV and  $M_\phi = 1102(13)_{\text{stat}}(-97)_{\text{sys}}$  MeV, where the systematic error is estimated by including a higher order term  $d_{\omega(\phi)}m_l^{3/2}$  [4] and by using a different input  $M_\Omega$  to fix the lattice spacing. These results are consistent with the experimental values  $M_\omega = 783$  MeV and  $M_\phi = 1019$  MeV. Note, however, that our data may suffer from significant finite volume corrections at two smallest quark masses  $m_l = 0.015$  and  $0.025$ , where  $2.8 \leq M_\pi L \leq 3.2$ . We are planning to extend this work to a larger volume  $24^3 \times 48$  for a more precise comparison with the experiment.

## 5. PS mesons

Figure 5 shows correlators of the light and strange PS mesons. In contrast to the vector mesons, the off-diagonal correlators  $G_{P,\{ls,sl\}}$  are not so small compared to the diagonal ones  $G_{P,\{ll,ss\}}$  in the light-strange basis. This leads to a significant strange (light) quark component in  $\eta$  ( $\eta'$ ). For the local operators, we obtain

$$\eta = 0.96(1)P_l - 0.28(3)P_s, \quad \eta' = 0.28(3)P_l - 0.96(1)P_s. \quad (5.1)$$

As in phenomenological analyses [5], more unambiguous determination of the mixing matrix could be provided by constructing the local  $\eta$  and  $\eta'$  operators so that their decay constants reproduce the experimental values. We leave this for a future study.

As predicted analytically [6] and as seen in Figs. 2 and 5, disconnected contribution  $D_{P,ab}$  induces a constant term in the full correlator  $G_{P,ab}$  at fixed topology, *e.g.*

$$m_l G_{P,ll} \xrightarrow{\Delta t \rightarrow \infty} \frac{\chi_t}{V} \left( 1 - \frac{Q^2}{\chi_t V} + \frac{c_4}{2\chi_t^2 V} \right), \quad (5.2)$$

which is suppressed by  $1/V$ . While this term is useful to determine the topological susceptibility  $\chi_t$  [7], this forces us to use  $G_{P,ab}$  at small  $\Delta t$  to extract the PS meson masses  $M_\eta$  and  $M'_{\eta'}$ .

To eliminate excited state contamination at such small  $\Delta t$ , we solve the GEVP with the  $10 \times 10$  correlator matrix including the smearing degrees of freedom

$$C(\Delta t) = \begin{pmatrix} G_{P,88,00}(\Delta t) & \cdots & G_{P,80,04}(\Delta t) \\ \cdots & \cdots & \cdots \\ G_{P,08,40}(\Delta t) & \cdots & G_{P,00,44}(\Delta t) \end{pmatrix}. \quad (5.3)$$

Effective masses of  $\eta$  and  $\eta'$  mesons are plotted in Fig. 6. Although  $\eta$  seems to be lighter than  $\eta'$ , the existence of the constant term in Eq. (5.2) leads to a large uncertainty of  $M_{\eta'}$ : 10–15% already at simulated quark masses.

From a linear chiral extrapolation in terms of  $m_l$  and  $m_s$ , we obtain  $M_\eta = 639(50)_{\text{stat}}$  MeV and  $M_{\eta'} = 840(136)_{\text{stat}}$  MeV at the physical point. These are consistent with the experimental values  $M_\eta = 548$  MeV and  $M_{\eta'} = 958$  MeV, though the statistical significance of the  $\eta' - \eta$  mass splitting ( $1.4 \sigma$ ) is not sufficient.

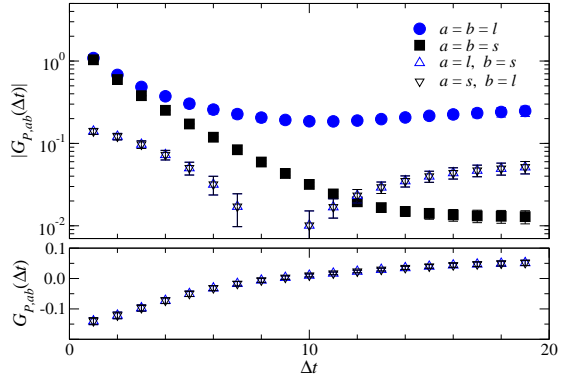


Figure 5: Light and strange PS meson correlators.

## 6. Conclusion

In this article, we report on our study of the flavor-singlet mesons in  $N_f=2+1$  lattice QCD using the all-to-all quark propagator to calculate the disconnected correlators. For the vector meson, we observe that the small disconnected contributions in the light-strange basis lead to the almost ideal mixing and the small mass shift. This is consistent with the experimental fact  $M_\omega \sim M_\rho$ , and explains why the previous calculations of  $M_\phi$  ignoring the disconnected contributions show reasonable agreement with experiment [8].

We need to improve the accuracy of  $M_{\eta'}$  to establish the  $\eta' - \eta$  mass splitting. This could be done by simulating non-trivial topological sectors as well as by suppressing the fixed topology effects in Eq. (5.2) on a larger lattice. The latter is also important to suppress finite volume corrections to the PS and vector meson masses for a more detailed comparison with the experiment. Such simulations on a  $24^3 \times 48$  lattice are in progress.

Numerical simulations are performed on Hitachi SR11000 and IBM System Blue Gene Solution at High Energy Accelerator Research Organization (KEK) under a support of its Large Scale Simulation Program (No. 09-05). This work is supported in part by the Grant-in-Aid of the Ministry of Education (No. 19740121, 20105001, 20105002, 20105003, 20105005, 20340047, 21105508, 21674002 and 21684013), the National Science Council of Taiwan (No. NSC96-2112-M-002-020-MY3, NSC96-2112-M-001-017-MY3, NSC97-2119-M-002-001), and NTU-CQSE (No. 97R0066-65 and 97R0066-69). The work of HF was supported by the Global COE program of Nagoya University "QFPU" from JSPS and MEXT of Japan.

## References

- [1] J. Foley *et al.* (TrinLat collaboration), *Comput. Phys. Commun.* **172**, 145 (2005).
- [2] H. Fukaya *et al.*, *Phys. Rev. D* **74**, 094505 (2006).
- [3] H. Matsufuru *et al.* (JLQCD and TWQCD collaborations), *PoS LATTICE2008*, 077 (2008).
- [4] E. Jenkins, A.V. Manohar and M.B. Wise, *Phys. Rev. Lett.* **75**, 2272 (1995).
- [5] For a recent analysis, see F. Ambrosino *et al.* (KLOE collaboration), *JHEP* **0907**, 105 (2009).
- [6] S. Aoki, H. Fukaya, S. Hashimoto and T. Onogi, *Phys. Rev. D* **76**, 054508 (2007).
- [7] S. Aoki, *et al.* (JLQCD and TWQCD collaborations), *Phys. Lett.* **B665**, 294 (2008).
- [8] For a recent review, see E. Scholz in these proceedings.

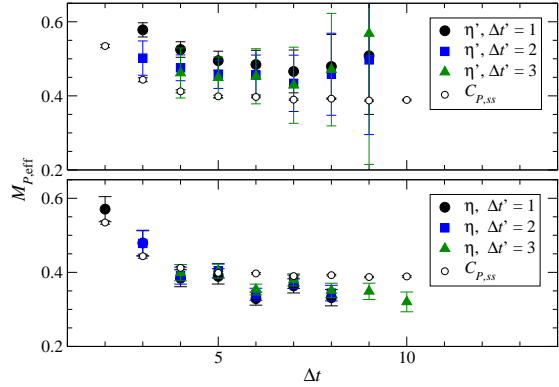


**Figure 6:** Effective masses of  $\eta'$  (top panel) and  $\eta$  (bottom panel) at  $(m_{ud}, m_s) = (0.025, 0.080)$  with different choices of  $\Delta t'$ . For a comparison, we also plot effective mass from the connected strange correlator  $C_{P,ss}$ .